ISSN 1070-3632, Russian Journal of General Chemistry, 2010, Vol. 80, No. 6, pp. 1078–1085. © Pleiades Publishing, Ltd., 2010.
Original Russian Text © V.E. Matulis, D.M. Palagin, O.A. Ivashkevich, 2010, published in Zhurnal Obshchei Khimii, 2010, Vol. 80, No. 6, pp. 908–915.

Theoretical Study of Optical Properties of Gold Clusters

V. E. Matulis, D. M. Palagin, and O. A. Ivashkevich

Research Institute of Physicochemical Problems of Belarus State University,
ul. Leningradskaya 14, Minsk, 220030 Belarus
e-mail: Vitaly_Matulis@mail.ru

Received January 14, 2010

Abstract—Characteristics of photoelectron spectrum of Au^{2-} and Au^{4-} clusters were calculated using different functionals and basis sets, and the results were compared with experimental data. The TD-B3LYP/LANL2Z method was shown to provide for calculation of these characteristics with good accuracy. Based on these results we suggested the methods and carried out appropriate calculations of the absorption and emission for different isomers of Au_8 clusters. It was shown that the best agreement with the experimental data is observed for the planar C_{2v} "hexagon+1" structure, therefore, this is the structure observed experimentally. The calculated value of the Stokes shift for the specified structure does not exceed 12 nm, which is also in good agreement with experimental results.

DOI: 10.1134/S1070363210060071

A great interest in the investigation of metal clusters is due to their unique properties that differ significantly from those of the bulk sample. In addition, the properties of clusters depend strongly on their size and shape, which holds great promise for the use of such structures in various fields of science, industry and medicine [1–6]. Particular attention, in connection with the possible use of other optical systems as new materials for sensors [4–8], attracted such unique optical properties of clusters as the luminescence. Recently a phenomenon was discovered of photoluminescence of nanosized gold particles and gold(I) complexes in the visible [7] and near infrared [9] regions of the spectrum.

In the present work we carried out a theoretical study of photoelectron spectra and luminescence of gold clusters in the framework of the density functional theory (DFT). A method for theoretical simulation of the absorption and emission spectra was proposed, and calculations of these spectra for the Au_8 cluster were performed. The results of calculations were compared with experimental data provided by Prof. Shinji Nozaki (Tokyo University of Electric communications, Tokyo, Japan). By comparison of the calculated and experimental data the structure of the Au_8 cluster was established whose luminescent properties were observed experimentally.

Features of calculation of photoelectron and luminescene spectra. The procedure of quantum chemical calculations of the lines in the luminescence spectra is very similar to that of calculating the photoelectron spectrum (PES) [10]. Thus, to calculate the position of the lines in the spectra in both cases the same methods may be applied: TD-DFT [11], CI [12], and CASSCF [13]. These methods allow the calculation of the energy of electronic transitions in the molecule (cluster) from the ground to the different excited states. For the calculation of metal clusters the method of DFT is preferred [10].

We, however, have to point out the two significant differences in the procedure for calculating the spectra of luminescence and PES.

First, in both cases the calculation of the electronic transition energy should be preceded by geometry optimization. For calculating the PES, like the case of absorption spectrum, it is necessary to optimize the geometric parameters of molecules in the ground electronic state, whereas for the calculation of emission spectrum the geometry optimization should be carried out for the singlet excited state of the molecule.

Second, at the calculation of PES is not necessary to take into account the selection rules. At the same time, at the calculation of absorption spectrum, as well as emission spectrum, selection rules should be considered.

In a general case, the intensity of the lines in the absorption spectrum is higher the higher the value of the dipole moment of transition between the ground and excited states. At the moment, in principle, there is no method for the accurate calculation of the transition dipole moments even for the simplest molecules. Consequently, we can estimate the intensity of the lines only qualitatively.

Photoelectron spectra of gold clusters. Since the procedure for calculating the photoelectron spectra and luminescence spectra are similar, then, before the theoretical modeling the luminescence spectra, we investigated the applicability of various levels of theory for calculating the characteristics of PES of the gold clusters. We calculated the PES for Au^{2-} and Au^{4-} using different combinations of the functional and the basis set, and compared the results with the experimental data [14]. Assuming that the first peak in the PES characterizes the vertical electron detachment energy for the anion cluster (VDE), its position was calculated as the difference between the total energy of the ground electronic state of the anionic cluster with optimum geometry and the electronic ground state of neutral cluster with the geometry of the anion. Subsequent lines in the photoelectron spectrum correspond to vertical transitions of the neutral cluster with the geometry of the anion from the ground to excited states (T_e). We calculated energies of these transitions by the method of TD-DFT. In the calculations of PES we used the following levels of theory: B3LYP [15]/LANL2DZ [16], B3LYP/SDD [17], B3PW91 [18]/LANL2DZ, PBEPBE [19]/ LANL2DZ, PBEPBE/SDD, S2LYP [20]/LANL2DZ , S2LYP/SDD, and LSDA [21]/LANL2DZ. On the basis of these studies we concluded that the best agreement between the calculated and experimental data for gold clusters was observed in the case of B3LYP functional with LANL2DZ basis set. Table 1 shows the results of (B3LYP/LANL2DZ) calculation and the experimental characteristics of PES of Au^{2-} and Au^{4-} clusters. As can be seen from Table 1, the use of the theory of B3LYP/LANL2DZ level allows the calculation of the position of lines in the PES of anionic gold clusters with a good accuracy. However, the calculated values of T_e (except T_{e1}) are slightly overestimated compared with experiment. Thus, in the case of the gold dimer, the calculated values of T_{e2}, T_{e3} and T_{e4} are by 0.12, 0.01 and 0.14 eV, respectively higher than the experimental ones. As in the case of Au^{2-}, for Au^{4-} all the calculated T_e correspond to

Table 1. Calculated and experimental characteristics of the photoelectron spectrum of clusters Au^{2-} and Au^{4-}, eV

Transition in PES	Au_2^-		Au_4^-	
	B3LYP/ LANL2DZ	experiment [14]	B3LYP/ LANL2DZ	experiment [14]
VDE	2.13	2.01	2.74	2.78
T_{e1}	1.55	1.59	0.53	0.64
T_{e2}	2.13	2.01	1.66	1.54
T_{e3}	2.25	2.24	1.86	1.66
T_{e4}	2.51	2.37	2.14	2.01

electronic transitions from the singlet ground state to the triplet excited state. For Au^{2-} cluster the values of T_{e1}, T_{e2}, T_{e3} and T_{e4} in the one-determinant approximation correspond to transitions of electrons to the lowest unoccupied molecular orbital (LUMO) from the respective highest occupied molecular orbital (HOMO): HOMO-1, HOMO-2,3 (degenerate states), and HOMO-4,5 (degenerate states). The forms of molecular orbitals (MO) and notation of the transitions between them are shown in Fig. 1. As seen from Fig. 1, transitions T_{e2}, T_{e3}, and T_{e4} are mainly from the molecular orbitals formed by the gold 5*d*-atomic orbitals (AO), and only to the T_{e1} transition contribute the orbitals formed by the gold 6s-AO. For the Au^{4-} cluster, the T_{e1}, T_{e2}, and T_{e3} transition in the one-determinant approximation correspond to electronic transitions HOMO–LUMO, HOMO–LUMO+1, and HOMO-1–LUMO. To the excited state corresponding to the transition T_{e4} contribute significantly several configurations at once, therefore it should not be considered as a single-electron transition. Figure 2 shows the shape of the molecular orbitals and transitions between them for the Au^{4-} cluster.

Experimental luminescence spectrum of Au_8. Recently, a group of researchers from the Tokyo University of Electric Communications (Tokyo, Japan) headed by Prof. Shinji Nozaki has conducted experimental studies of the absorption and emission of Au_8 cluster (Fig. 3). The black lines (A_1 and A_2) in Fig. 3 correspond to the absorption spectra of solution of the gold clusters obtained directly after synthesis, and the clusters after treatment with ion exchange resin

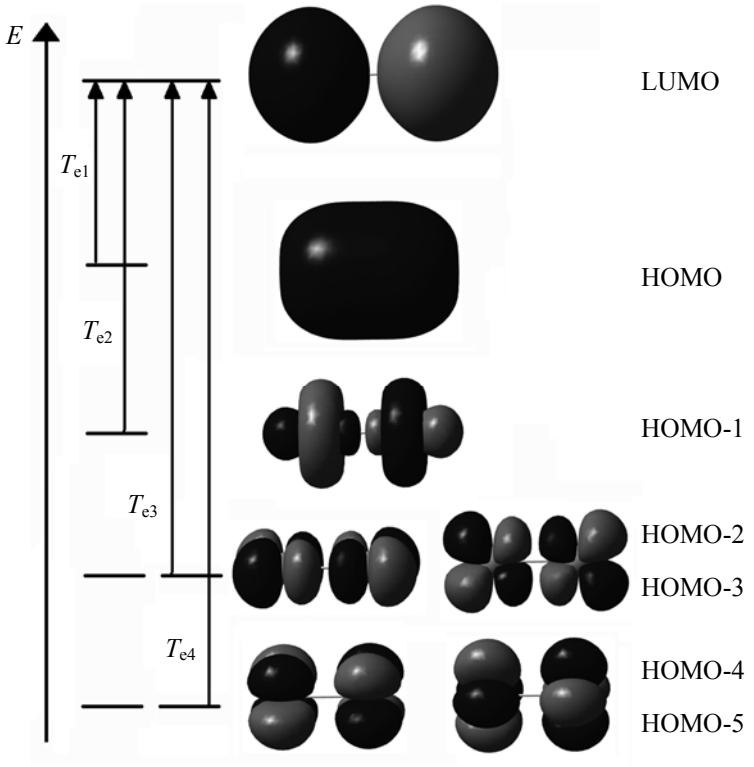

Fig. 1. Forms of MO and notations of the transitions between them in the PES of Ag_2^-.

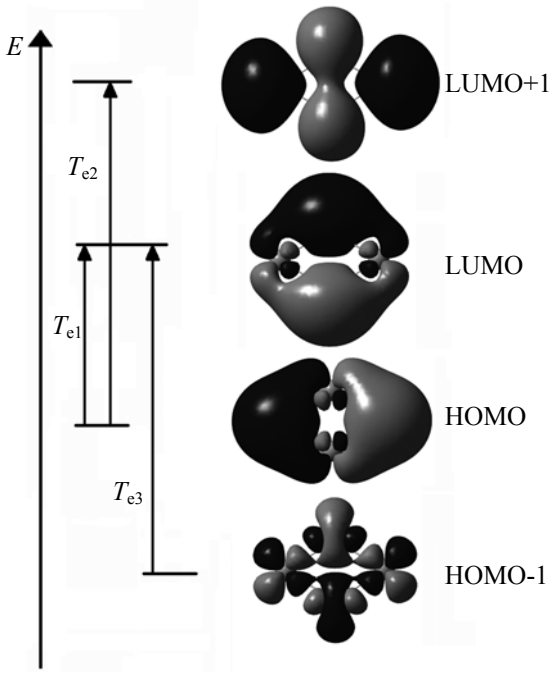

Fig. 2. Forms of MO and notations of the transitions between them in the PES of Ag_4^-.

to remove surfactant. In the spectra there are three peaks corresponding to wavelengths of transitions 375.5 nm, 257.2 nm, and 226.4 nm. To the emission spectra of the solution after the synthesis, and after treatment with ion exchange resin correspond lines E_1 and E_2, respectively. The main peak in the emission spectrum in both cases is quite close to that in the absorption spectrum. Consequently, the value of the Stokes shift is small (11.5 nm for the first solution and is close to zero for the second).

Calculation of absorption spectrum of Au_8 cluster. There are a lot of mutually consistent data on the structure of the Au_8 cluster [22–24]. According to these data, the most stable are the structures shown in Fig. 4. Taking into account the data of [22–24], we calculated the absorption spectra of six isomers of Au_8 cluster: the planar star D_{4h} structure, the planar C_{2v} "hexagon+1" structure, the planar C_{2v} "boat" structure, the three-dimensional D_{2d} structure, the three-dimensional tetrahedral (T_d) structure, and the three-dimensional C_{2v} pyramidal structure (Fig. 4).

With our results on PES of Au^{2-} and Au^{4-} we calculated the absorption spectra using functional B3LYP with the basis set LANL2DZ. Procedure for

the calculation of the absorption spectrum included the following stages. First of all, the geometry optimization of the cluster in the ground electronic state was carried out. As a result of the geometry optimization five structures were obtained as the three-dimensional D_{2d} structure transformed into a more stable tetrahedral one. Table 2 shows the relative energies of the structures obtained.

Further, for the optimized structures energies of electronic transitions were calculated by TD-B3LYP/LANL2DZ. As the result of calculation the energies of electronic transitions and the corresponding transition dipole moments were obtained. Note that the transition intensity depends on the corresponding dipole moment. The absorption spectrum was simulated by representing each line with a Gaussian curve with a given width at half-height:

$$I(\lambda) = \sum_i f_i \exp\{-1/2[(\lambda - \lambda_1)/\sigma]^2\},$$

where σ is the width of the peak i at the wavelength λ_i with the transition dipole moment f_i.

Figures 5 and 6 show the theoretically calculated absorption spectra of different isomers of Au_8 cluster, as well as the relevant optimized geometric structures. By comparing the calculated spectra (Figs. 5, 6) with the experimental absorption spectrum (Fig. 3) we can conclude that the best agreement with the experiment is observed in the case of the flat "hexagon+1" structure (Fig. 5). Comparison of positions of the major peaks in the calculated and experimental

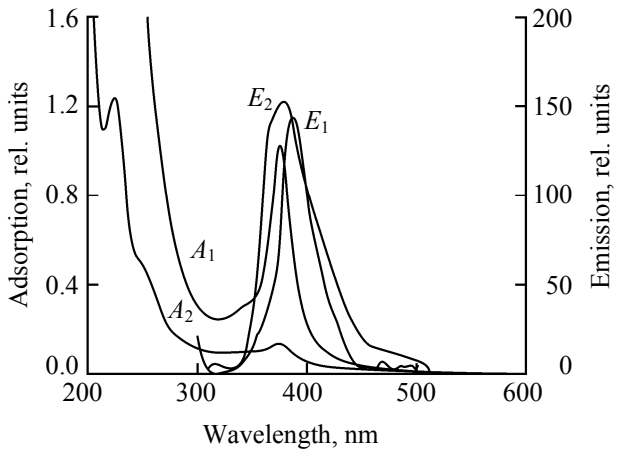

Fig. 3. Experimental [22] absorption and emission spectra of of Au_8 cluster. A_1 and A_2 are the lines in the absorption spectra of solution of gold clusters, obtained directly after synthesis, and clusters after treatment with ion exchange resin, respectively. E_1 and E_2 are the lines in the emission spectra of the solution obtained in the synthesis and after treatment with ion exchange resin, respectively.

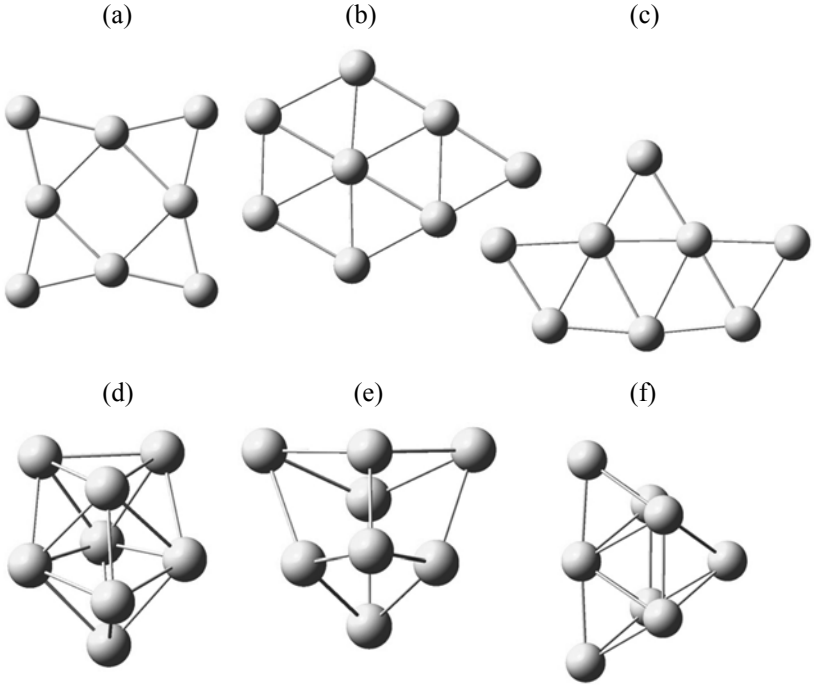

Fig. 4. The most stable [23–25] structures of the Au_8 clusters, whose geometric parameters were optimized in this work: (a) flat star structure (D_{4h}), (b) flat "hexagon +1" (C_{2v}) structure, (c) flat boat (C_{2v}) structure, (d) three-dimensional D_{2d} structure, (e) three-dimensional tetrahedral (T_d) structure, and (f) three-dimensional pyramidal (C_{2v}) structure.

Table 2. Relative B3LYP/LANL2DZ energies of the optimized structures of the Au_8 cluster

Structure no. (see Fig. 4)	Structure	Relative energy, eV
1	flat star	0.00
2	flat "hexagon+1"	0.54
3	flat boat	0.71
5	three-dimensional tetrahedral	0.78
6	three-dimensional pyramid	0.75

Table 3. Calculated (B3LYP/LANL2DZ) and experimentally observed [22] peaks in the absorption spectrum of the Au_8 cluster

Peak no.	Peak position, nm	
	calculated	experiment [22]
1	371.3	375.5
2	278.7	257.2
3	233.1	226.4

absorption spectra is given in Table 3. The data of Table 3 show that the results of calculation for the "hexagon+1" structure are in good agreement with experimental data. It should be noted that the wave function of the excited state differs significantly from the wave function of the ground state. The difference is the greater the higher the energy of the transition. Therefore, the deviation of calculated values of the lines in the spectrum from the experimental ones is larger for the transitions with lower wavelengths. Thus, comparing the calculated and experimental data we can state that in the experimental studies conducted by Prof. Shinji Nozaki and co-workers was observed the C_{2v} isomer "hexagon +1."

Calculation of emission spectrum of the Au_8 cluster. Since the best agreement of theoretically calculated and experimental absorption spectra is observed in the case of the flat structure "hexagon+1" (see Table 3), the emission spectrum was calculated specifically for this structure.

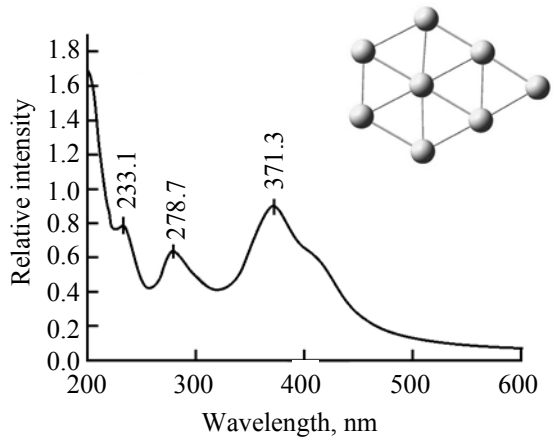

Fig. 5. Calculated absorption spectrum for the flat structure of the Au_8 cluster "hexagon+1" using the level of theory B3LYP/LANL2DZ.

To estimate the Stokes shifts we calculated characteristics of the emission spectrum using two methods. In the first method, initially the optimization of the first excited state of the flat "hexagon+1" structure at the level of theory CIS/LANL2DZ was carried out. Then for the structure obtained as a result of the optimization TD-B3LYP/LANL2DZ calculation was carried out of the lines in the emission spectrum. In the future this method of calculation will be denoted as CIS/LANL2DZ//TD-B3LYP/LANL2DZ. In the framework of the second method, both the optimization of the first excited state and the calculation of the lines in the emission spectrum were carried out by TD-B3LYP/LANL2DZ method. This method requires more computational resources, but is more reliable. The emission spectra of Au_8 cluster calculated under the described approximations are shown in Fig. 7. Changes in the geometric characteristics of the cluster in the excited state compared to the ground state are shown in Fig. 8. In Fig. 9 the calculated absorption spectrum is compared with the emission spectra calculated in two approximations that allows the estimation of the value of the Stokes shift. As seen from Fig. 7, the positions of peaks in the emission spectrum calculated by both methods are in good agreement with each other. The nature of the distortion of the cluster structure at the excitation predicted in the two approximations is also the same (Fig. 8). It should be noted that, according to calculations, the distortion of the cluster geometry at the transition to an excited state is small.

Comparison of the calculated values of the Stokes shift with the experimental data suggests that TD-B3LYP/LANL2DZ method gives better agreement with experiment than CIS/LANL2DZ//TD-B3LYP/LANL2DZ. Thus, the value of Stokes shift calculated by TD-B3LYP/LANL2DZ does not exceed 11.5 nm.

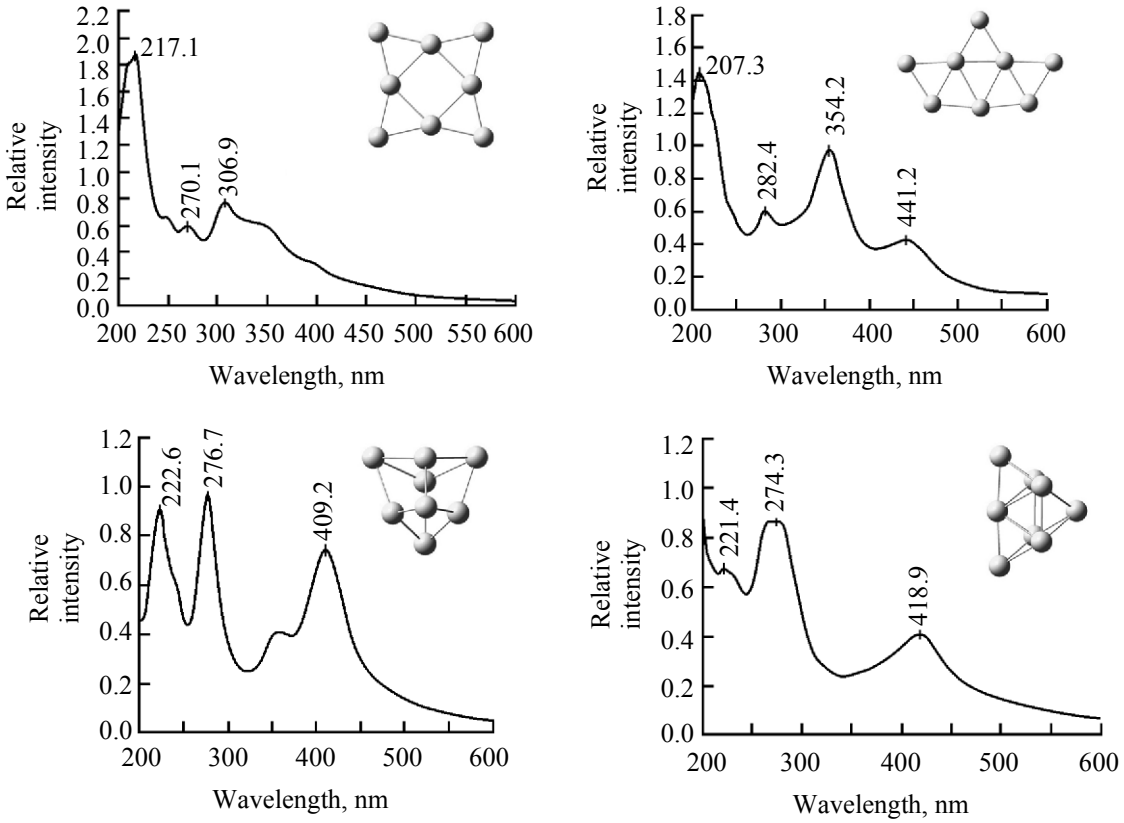

Fig. 6. Calculated absorption spectra of four isomers of Au_8 cluster using the level of theory B3LYP/LANL2DZ.

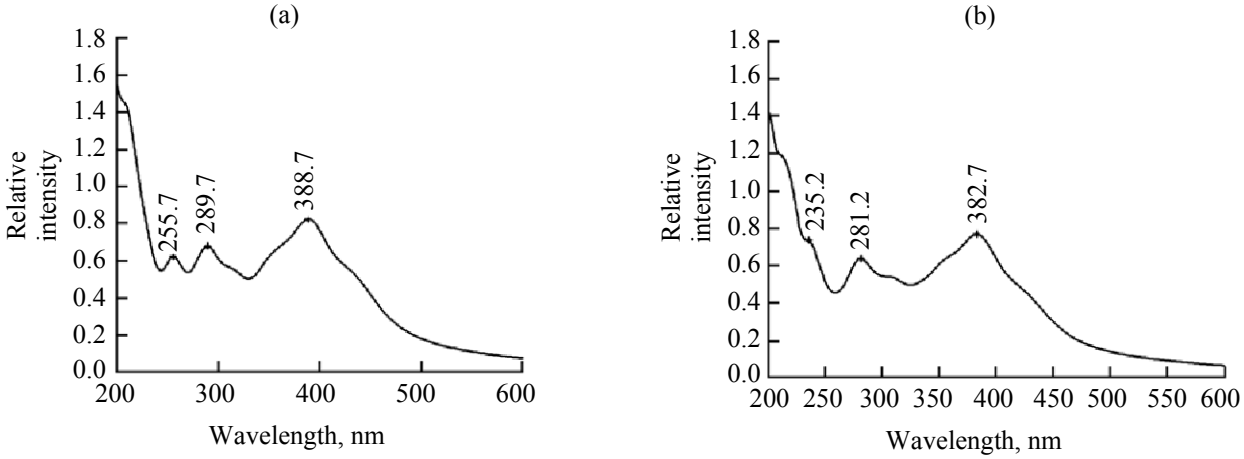

Fig. 7. Calculated by (a) CIS/LANL2DZ, TD-B3LYP/LANL2DZ and (b) TD-B3LYP/LANL2DZ emission spectra of the Au_8 cluster "hexagon+1" using the level of theory B3LYP/LANL2DZ.

The relatively small Stokes shift is explainable by only slight distortion of the geometric structure of the cluster at the excitation.

Thus, comparison of calculated and experimental characteristics of PES of the gold clusters shows that the method TD-B3LYP/LANL2DZ allows to calculate the energy of electronic transitions with high precision and can be used for theoretical modeling of the luminescence spectra of gold clusters.

The calculations of the absorption spectra of five isomers of Au_8 shows that the best agreement with experiment is observed for the planar C_{2v} "hexagon+1"

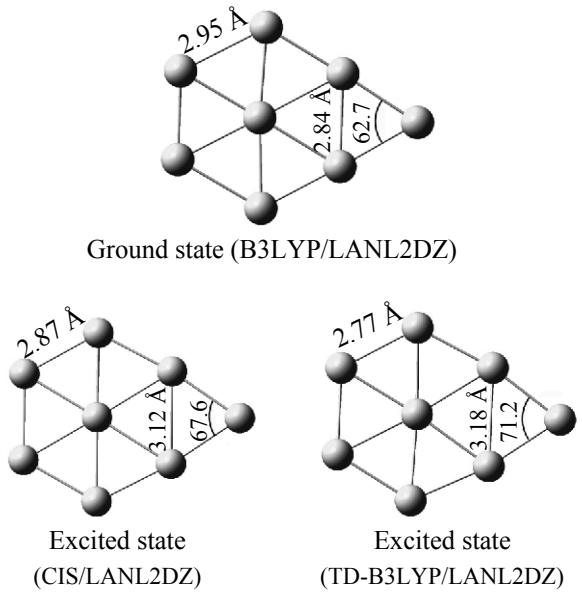

Fig. 8. Change in the geometric parameters of the cluster in the excited state compared to the ground state.

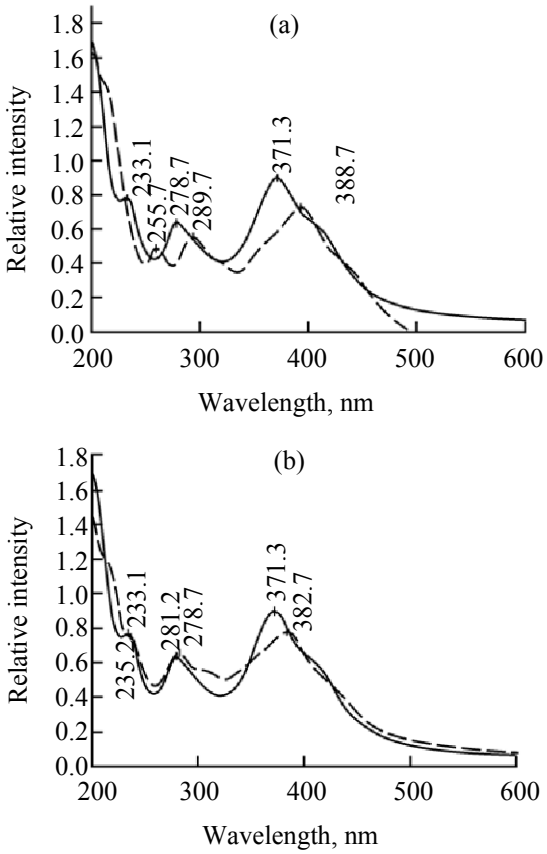

Fig. 9. Absorption and emission spectra of Au_8 cluster. The solid line corresponds to the absorption spectrum, dashed to the emission spectrum. (a) Emission spectrum calculated by CIS/LANL2DZ, TD-B3LYP/LANL2DZ and (b) emission spectrum calculated by TD-B3LYP/LANL2DZ.

structure. Comparison of the data calculated for this structure for the emission and absorption spectra allows us to conclude that the observed Stokes shift is small in agreement with the experimental results. Thus, it can be stated that in the experimental studies conducted by Prof. Shinji Nozaki and co-workers the C_{2v} "hexagon+1" isomer has been observed.

ACKNOWLEDGMENTS

The authors are grateful to Professor Shinji Nozaki and Satchidananda Rath (Department of Electronic Engineering, The University of Electro-Communication, Tokyo, Japan) for providing the experimental data on the spectra of Au_8 cluster.

REFERENCES

1. Li, J., Li, X., Zhai, H.J., and Wang, L.S., *Science,* 2003, vol. 299, p. 864.
2. Walter, M., Frondelius, P., Honkala, K., and Hakkinen, H., *Phys. Rev. Lett*., 2007, vol. 99, p. 096102.
3. Sengupta, B., Ritchie, C.M., Buckman, J.G., Johnsen, K.R., Goodwin, P.M., and Petty, J.T., *J. Phys. Chem., C,* 2008, vol. 112, p. 18776.
4. Huang, S.Y., Huang, C.D., Chang, B.T., and Yeh, C.T., *J. Phys. Chem., B*, 2006, vol. 110, p. 21783.
5. Yoon, B., Hakkinen, H., Landman, U., Worz, A.S., Antonietti, J.M., Abbet, S., Judai, K., and Heiz, U., *Science*, 2005, vol. 307, p. 403.
6. Peyser, L.A., Vinson, A.E., Bartko, A.P., and Dickson, R.M., *Science*, 2001, vol. 291, p. 103.
7. Zheng, J., Zhang, C., and Dickson, R.M., *Phys. Rev. Lett*., 2004, vol. 93, p. 077402.
8. Zheng, J., Petty, J.T., and Dickson, R.M., *J. Am. Chem. Soc*., 2003, vol. 125, p. 7780.
9. Link, S., Beeby, A., Fitzgerald, S., El-Sayed, M.A., Schaaff, T.G., and Whetten, R.L., *J. Phys.Chem., B,* 2002, vol. 106, p. 3410.
10. Matulis, V.E., Ivashkevich, O.A., and Gurin, V.S., *J. Mol. Struct., (Theochem.)*, 2003, vols. 664–665, p. 291.
11. Stratmann, R.E., Scuseria, G.E., and Frisch, M.J., *J. Chem. Phys*., 1998, vol. 109, p. 8218.
12. Foresman, J.B., Head-Gordon, M., Pople, J.A., and Frisch, M.J., *J. Phys. Chem*., 1992, vol. 96, p. 135.
13. Li, J.-Q, Li, X.-Y., and Wang, F., *J. Theor. and Comput. Chem*., 2008, vol. 7, p. 821.
14. Handschuh, H., Ganteför, G., Bechthold,P.S., and Eberhardt, W., *J. Chem. Phys*., 1994, vol. 100, p. 7093.
15. Becke, A.D., *J. Chem. Phys*., 1993, vol. 98, p. 5648.
16. Hay, P.J. and Wadt, W.R., *J. Chem. Phys*., 1985, vol. 82, p. 299.

17. Andrae, D., Haussermann, U., Dolg, M., Stoll, H., and Preuss, H., *Theor. Chim. Acta*, 1990, vol. 77, p. 123.
18. Perdew, J.P., *Phys. Rev., B*, 1986, vol. 33, p. 8822.
19. Perdew, J.P., Burke, K., and Ernzerhof, M., *Phys. Rev. Lett*., 1996, vol. 77, p. 3865.
20. Matulis, V.E., Ivashkevich, O.A., and Gurin, V.S., *J. Mol. Struct. (Theochem.),* 2004, vol. 681, p. 169.
21. Vosko, S.H., Wilk, L., and Nusair, M., *Can. J. Phys*., 1980, vol. 58, p. 1200.
22. Han, Y.K., *J. Chem. Phys*., 2006, vol. 124, p. 024316.
23. Olson, R.M. and Gordon, M.S., *J. Chem. Phys*., 2007, vol. 126, p. 214310.
24. Diefenbach, M. and Kim, K.S., *J. Phys. Chem., B*, 2006, vol. 110, p. 21639.